

# Maser Effects in Recombination Lines: the case of Eta Carinae

Zulema Abraham<sup>1</sup>, Pedro P. B. Beaklini<sup>1</sup> and Diego Falceta-Gonçalves<sup>2</sup>

<sup>1</sup>Instituto de Astronomia, Geofísica e Ciências Atmosféricas, Universidade de São Paulo, Rua do Matão 1226, 05508-090, São Paulo, SP, Brazil.  
email: zulema.abraham@iag.usp.br

<sup>2</sup>Escola de Artes, Ciências e Humanidades, Universidade de São Paulo, R. Arlindo Bettio 1000, 03828-000, São Paulo, SP, Brazil

**Abstract.** Population of high quantum number states can differ from their LTE values at high densities ( $\text{Ne} \sim 10^6 - 10^8 \text{ cm}^{-3}$ ) and temperatures of the order of  $10^4 \text{ K}$ . In this case, the intensity of recombination lines can be strongly amplified. The amount of amplification depends on density and temperature, and it is different for different quantum numbers, allowing the determination of the physical and kinematic conditions of the emitting region through the observation of recombination lines of different quantum numbers. This was the case of the massive binary system  $\eta$  Carinae. This system was observed with ALMA in the recombination lines  $\text{H}21\alpha$ ,  $\text{H}28\alpha$ ,  $\text{H}30\alpha$ ,  $\text{H}40\alpha$  and  $\text{H}42\alpha$  and the continuum at the frequencies of the corresponding lines. The continuum spectrum was characteristic of a compact HII region, becoming optically thin at around 300 GHz. From the intensity and width of the recombination lines we concluded that the not-resolved emission region, assumed spherically symmetric, is a shell of 40 AU radius and 4 AU width, expanding at velocities between 20 and 60  $\text{km s}^{-1}$ , with density of  $10^7 \text{ cm}^{-3}$  and temperature of 17000 K.

**Keywords.** masers, mass loss, stellar winds,  $\eta$  Carinae

---

## 1. Introduction

$\eta$  Carinae is one of the most massive stars in our Galaxy. It is possibly an LBV (Luminous Blue Variable) star that presented several episodes of mass ejection. The largest occurred in 1840, when it ejected  $\sim 12 M_{\odot}$  that formed the Homunculus Nebula, now expanding at about 600  $\text{km s}^{-1}$ . At that time, its optical magnitude reached  $-1$ , and after that its brightness decreased as the cloud expanded and dust formed. Another smaller episode of mass ejection occurred in 1890, and maybe a third one in 1942 (Fernández-Lajús *et al.* 2009).

$\eta$  Carinae is not a single star, but a binary system in a very eccentric orbit. The 5.52 yr periodicity in the X-ray light curve, observed by the RXTE (Corcoran *et al.* 2001), and also in the intensity of lines of highly ionized elements (Damineli 1996) and in continuum flux density at radio frequencies (Abraham *et al.* 2005), are proof of the binary nature of the system. The companion star has not been detected, because of absorption by the Homunculus and the strong wind of  $\eta$  Carinae. The secondary star must also have a wind, and the winds' collision produces a shock that emits at X-rays.

At radio frequencies it was mapped by Duncan, White & Lim (1997) at 5 GHz with the Australian Compact Array (ATCA). The maps resemble an edge-on disk, with an arc-like structure, which shrinks to a point-like source close to the dips in the X-ray light curve. Both regions are probably ionized by the companion star.

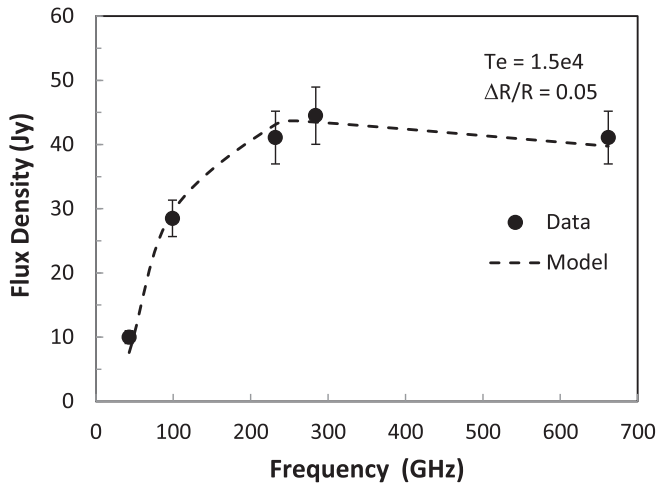


**Figure 1.** Interferometric continuum observations of  $\eta$  Carinae from ALMA and single dish (43GHz) from Itapetinga.

$\eta$  Carinae was also observed with SEST in the continuum at 1.3 and 3 mm, and at the recombination lines H29 $\alpha$ , H40 $\alpha$  and H50 $\beta$  (Cox *et al.* 1995a,b). The source was not resolved in the continuum and showed a spectrum that increased with frequency as  $S(\nu) \propto \nu^{0.6}$ ; its flux density also depended on the orbital phase. The recombination lines were asymmetric and strong, affected by NLTE effects. The continuum emission was attributed to the free-free process in the  $\eta$  Carinae wind. Further observations were made with SEST, between 1999 and 2003, in the continuum at 100, 150 and 230 GHz, as well as in the recombination lines H30 $\alpha$ , H35 $\alpha$  and H40 $\alpha$  (Abraham, Daminieli & Durouchoux 2002; Abraham *et al.* 2005). The observations required long integration times, especially for the continuum, and had uncertainties due to the lack of calibration sources and pointing corrections.

The continuum emission was also observed at 7 mm (43 GHz) with the Itapetinga radiotelescope, in Brazil, from 2003 to 2014 (Abraham *et al.* 2005).

## 2. Observations and Results

$\eta$  Carinae was observed with ALMA in Cycle 0, at four continuum bands, centered at 92, 225, 291 and 672 GHz, with resolutions of 2.8, 1.5, 0.8 and 0.45 arcsec, and in the recombination lines H42 $\alpha$ , H40 $\alpha$ , H30 $\alpha$ , H28 $\alpha$  and H21 $\alpha$  (Abraham, Falceta-Gonçalves & Beaklini 2014). The source was not resolved, neither in the continuum nor in the recombination lines.

The continuum spectrum is shown in Fig. 1. It includes 43 GHz single dish data from the Itapetinga radiotelescope in Brazil. As we can see, it is a typical spectrum of a compact HII region that becomes optically thin at a frequency of about 300 GHz.

In Fig. 2 we present the recombination line spectra. Notice the high intensity of the H lines and the presence of corresponding He lines.

In Fig. 3 we show the position vs. velocity diagram for the H28 $\alpha$  line, in the direction of the clean beam major axis. This diagram is typical of an expanding region and for that reason we modeled the source as a spherically symmetric expanding shell and solved the equations of radiative transfer for the continuum and lines, using the NLTE line emission coefficients calculated by Storey & Hummer (1995). The model parameters are: electron density  $N_e$  and temperature  $T_e$ , size  $R$  and width  $\Delta R$  of the shell, and bulk expansion

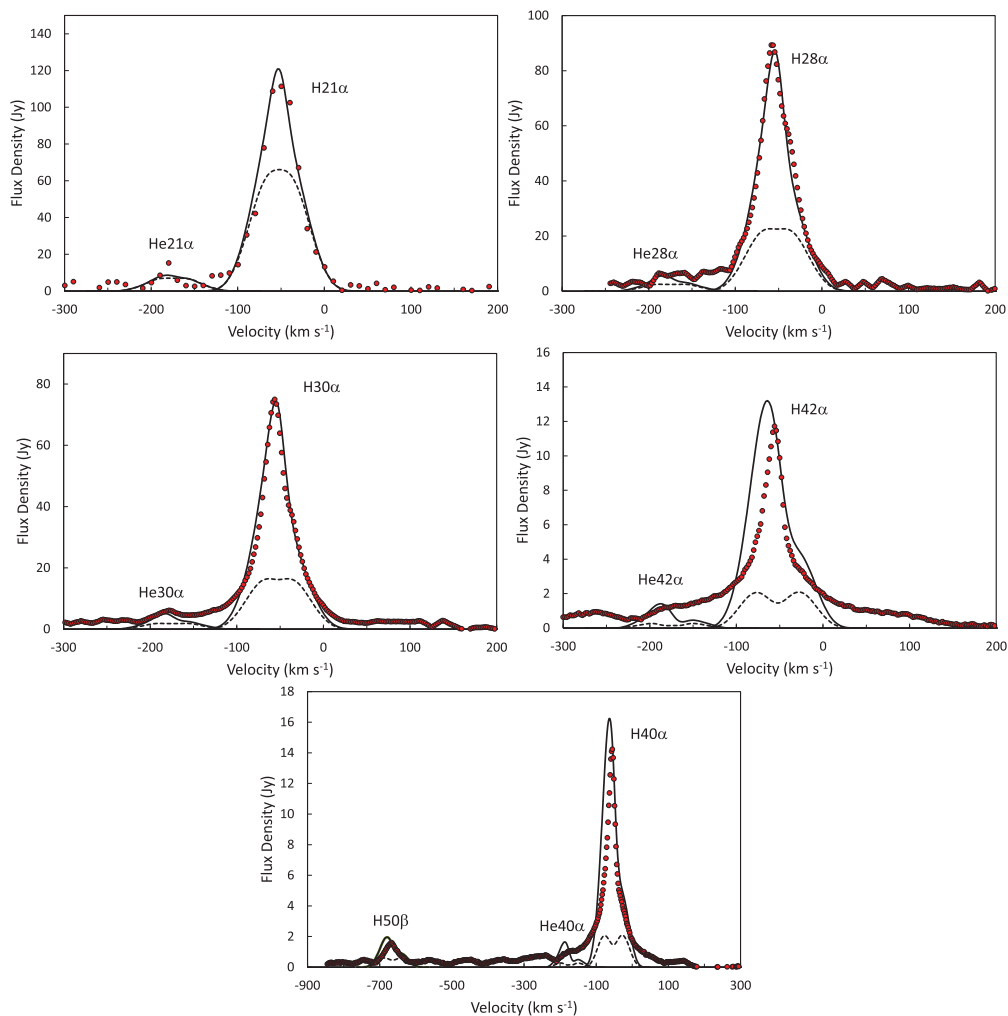


**Figure 2.** Recombination lines from  $\eta$  Carinae observed with ALMA (points). The continuum line represents the best fit to a NLTE model and the broken line the same model but considering LTE conditions

velocity  $v_0$  and its gradient across the shell (internal  $v_i$  and external  $v_e$  velocities). The parameters for which the best fit of the continuum and the line profiles are obtained are:  $N_e = 1.5 \times 10^7 \text{ cm}^{-3}$ ,  $T_e = 1.7 \times 10^4 \text{ K}$ ,  $R = 40 \text{ AU}$ ,  $\Delta R = 0.1R$ ,  $v_0 = -52 \text{ km s}^{-1}$ ,  $v_i = 60 \text{ km s}^{-1}$ ,  $v_e = 20 \text{ m s}^{-1}$ .

The model for the continuum emission is presented in Fig. 1 as a broken line and for the line profiles in Fig. 2 as continuous lines. We also modeled the corresponding He lines, the H50 $\beta$  line and the line profiles using LTE emission coefficients, which are shown as broken lines.

Since  $\eta$  Carinae is probably an LBV star, the compact shell can be the result of a recent mass ejection accompanied by a brightness variation, as that observed in the optical light curve in 1942 (Fernández-Lajús *et al.* 2009).

We are grateful to the Brazilian research agencies FAPESP and CNPq for financial support (FAPESP Projects: 2008/11382-3 and 2014/07460-0).

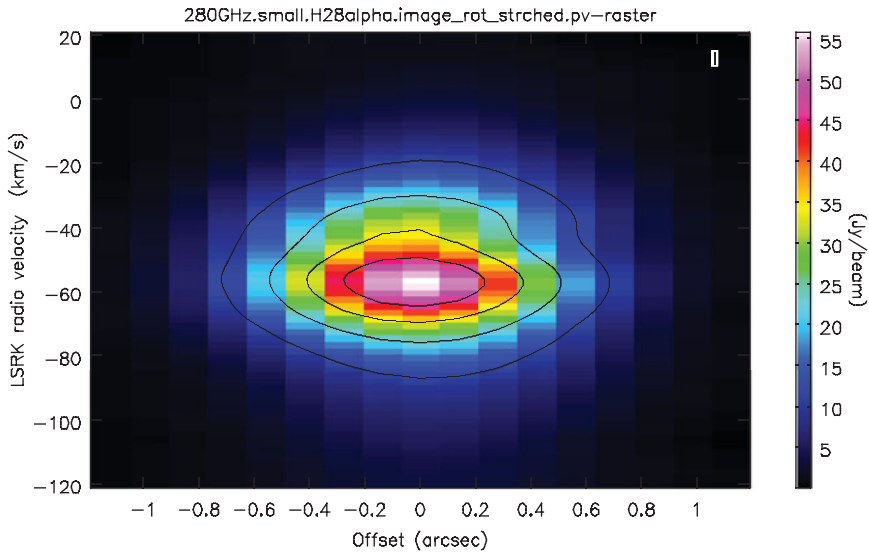


**Figure 3.** Position vs. velocity diagram for the H28 $\alpha$  line in the direction of the clean beam major axis. The contours are 0.2, 0.4, 0.6 and 0.8 of the maximum flux density, which is 55.9 Jy beam<sup>-1</sup>.

## References

- Abraham, Z., Daminieli, A., Durouchoux, P., in *Cosmic MASERS, from Protostars to Black Holes*, 2002, IAU Symposium 206, 234, ed. V. Migenes & M. J. Reid
- Abraham, Z., Falceta-Gonçalves, D., Dominici, T. M. *et al.*, 2005, *A&A*, 437, 997
- Abraham, Z., Falceta-Gonçalves, D., & Beaklini, P. P. B., 2014, *ApJ*, 791, 95
- Corcoran, M. F., Ishibashi, K., Swank, J. H., & Petre, R., 2001, *ApJ*, 547, 1034
- Cox, P. G., Martin-Pintado, J., Bachiller, R. *et al.*, 1995a, *A&A*, 295, L39
- Cox, P. G., Mezger, P. G., Sievers, A. *et al.*, 1995b, *A&A*, 297, 168
- Daminieli, A., 1996, *ApJ*, 460, L49
- Duncan, R. A., White, S. M., & Lim, J., 1997, *MNRAS*, 290, 680
- Fernández-Lajús, E., Farinã, C., Torres, A. F., *et al.*, 2009, *A&A*, 493, 1093
- Storey, P. J. & Hammer, D. G., 1995, *MNRAS*, 272, 41